

Faster-than-Nyquist DFT-S-OFDM using Overlapping Sub-Bands and Duobinary Filtering

Chen Zhu¹, Bill Corcoran^{1,2}, Monir Morshed^{1,2}, Leimeng Zhuang¹, and Arthur J. Lowery^{1,2}

¹Electro-Photonics Laboratory, Electrical and Computer Systems Engineering, Monash University, Australia

²Centre for Ultrahigh-bandwidth Devices for Optical Systems (CUDOS), Australia

Email: chen.zhu@monash.edu

Abstract: We propose a novel single-channel Faster-than-Nyquist-DFT-S-OFDM transmitter that allows the sub-bands' spectra overlap flexibly. By combing duobinary filtering to mitigate inter-sub-band interference, 12% more spectral efficiency is demonstrated in a super-channel experiment over 3360-km transmission.

OCIS codes: (060.1660) Coherent communications; (060.2330) Fiber optics communications.

1. Introduction

Nyquist-WDM [1] and orthogonal frequency division multiplexing (OFDM) [2] are two promising methods of achieving high spectral efficiencies, by allowing the spacing between the WDM channels/subcarriers to be reduced towards, or to, the baud rate. The channel spacing can be reduced further by accepting some inter-channel interference (ICI), giving rise to super-Nyquist or faster-than-Nyquist (FTN) systems [3, 4].

In all previous work, the FTN system is realized by using a channel spacing less than the baud rate [4]; that is, part of the spectrum is shared between adjacent channels; we will call this “multi-channel FTN”. Such a scheme is not flexible when adjusting the ICI according to different network scenarios. Also multi-channel FTN is sensitive to random drifts in laser frequency, since the channel spacing is set by the frequencies of the channel lasers.

In this paper, we show that using multi-band discrete-Fourier-transform spread OFDM (DFT-S-OFDM) [5], allows the overlapping parts of adjacent sub-bands (within a single-channel) to be created in a controlled manner, with the benefit to define zero ICI, even when FTN is used. This “FTN-DFT-S-OFDM” system allows the actual per-channel symbol rate beyond the Nyquist bandwidth with negligible extra computational effort, and is transparent to dynamic optical routing where channels are switched in and out of the network. Furthermore, well-established ICI mitigation techniques such as duobinary pulse shaping with MLSE detection [4, 6] can be implemented to suppress interference between the sub-bands, which can improve the receiver sensitivity significantly. The proposed concept is experimentally verified in a 14×38.4-Gb/s super-channel experiment over 3360-km transmission distance.

2. Generation and reception of FTN-DFT-S-OFDM

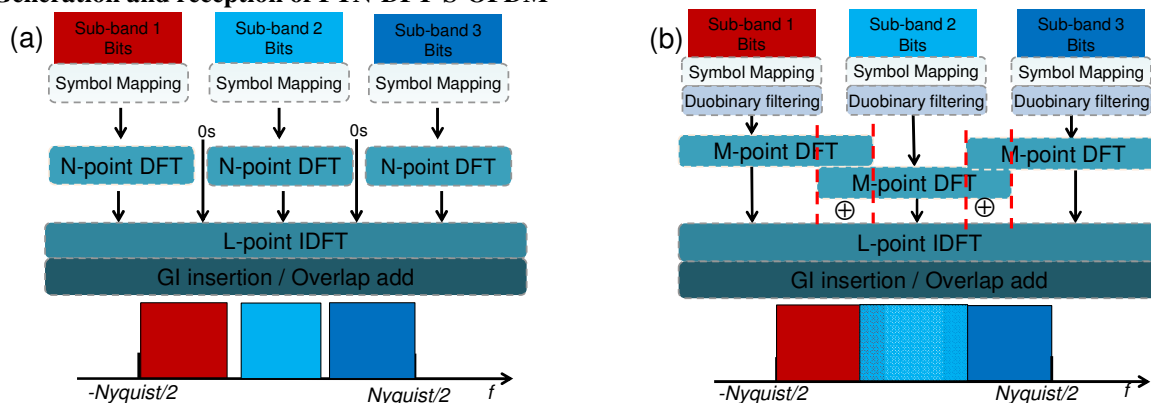


Fig. 1. Schematic diagram for generation of: (a) conventional DFTS-OFDM and (b) FTN-DFT-S-OFDM.

Figure 1 compares the transmitter digital signal processing (DSP) structure of conventional DFT-S-OFDM and FTN-DFT-S-OFDM systems. A three sub-band example is shown here, but the concept can be easily extended to many sub-bands. As shown in Fig. 1a, for conventional DFT-S-OFDM, in each sub-band a bit stream is modulated and converted to frequency domain by a N -point DFT, and then the three DFT outputs are mapped into a L -point IDFT. Zeros can be inserted between the adjacent sub-bands, to act as guard bands. After the IDFT, either overlap-add operation (overhead free) [7] or guard interval insertion (overhead required such as cyclic prefix) [5] can be chosen. With conventional DFT-S-OFDM, the DFT outputs of different sub-bands do not overlap one-another when mapped to the IDFT window, to allow de-multiplexing without a penalty due to inter-sub-band interference (ISBI).

The structure of our proposed FTN-DFT-S-OFDM is depicted in Fig. 1b. The major differences are that: (a) the signals are mapped into a larger DFT block sizes, and (b) portions of the DFTs' outputs are overlapped; therefore symbol rate is higher than the Nyquist bandwidth, leading to a single-channel FTN rate. Regarding computational complexity, the FTN-DFT-S-OFDM operation requires larger DFT size and extra adders which depends on the spectrum overlap ratio, but it accommodates more symbols each block, therefore the additional computational effort is negligible. The duobinary filtering is an optional functional block; it narrows the sub-band signal spectrum, and therefore mitigates the ISBI. Because all of the sub-bands can be captured simultaneously at the receiver, frequency diversity MIMO processing [8] could also be implemented, to mitigate ISBI.

3. Experimental demonstration

Figure 2a shows the experimental setup. QPSK modulation was used. The baseband signal was generated offline. Two sub-bands were used for easy visual comparison. For the conventional DFT-S-OFDM system, the DFT size was 812, with 12-zeros used for the guard band. The IDFT used 2048-points, to generate a spectrum with $1.25\times$ oversampling rate ($= 2048/(2\times 812+12)$). 50% percent overlap-add was used, instead of cyclic prefix insertion, to minimize the system overhead, *i.e.* 406 data symbols were mapped to each DFT block. For the FTN-DFT-S-OFDM system, most of the parameters were kept the same, but DFT size was set to 918/1018 for 12%/24% sub-band spectrum overlapping ratios (giving effective per-channel symbol rates of 9.6 Gbaud/11.2 Gbaud), respectively. Before upload to a 10-GSa/s arbitrary waveform generator (AWG), pre-equalization was performed to combat the frequency roll-off of the AWG.

To construct a 112-GHz super-channel from this single data modulator, the data modulator was fed with seven comb lines 16-GHz apart (inset (i) of Fig. 2a), generated by overdriving an optical intensity modulator then equalized using a Finisar Waveshaper (WS). The optical source was an Agilent external cavity laser (ECL). A half-filled spectrum was generated in this way. The generated optical spectra of the middle wavelength channel with conventional and FTN DFT-S-OFDM are depicted in Fig. 2b-f. It is clear that without duobinary filtering (Fig. 2b-d), the spectrum shows a larger plateau as the sub-band overlapping ratio increases; while when duobinary filtering is applied (Fig. 2e-f), a narrower sub-band is observed, *i.e.* the edge spectrum of each sub-band carries less information, which effectively mitigates the effect of ISBI even when the sub-bands overlap strongly.

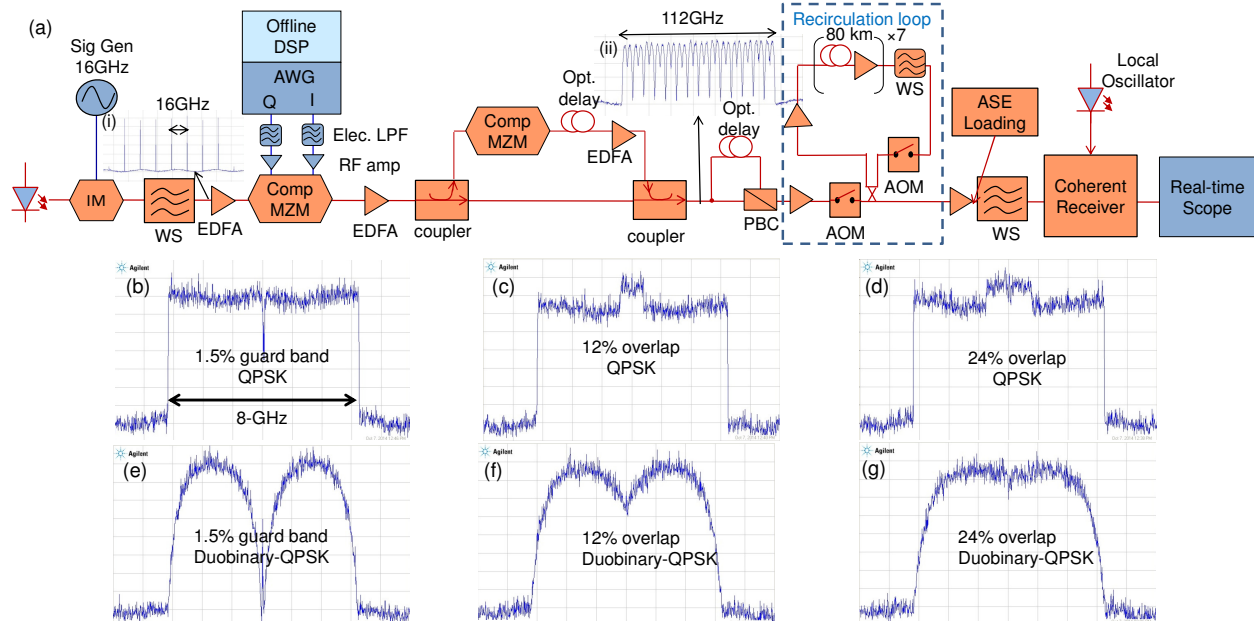


Fig. 2. (a): Experimental setup, PBC: polarization beam combiner, AOM: acousto-optic modulator; (b)-(g): Spectra of the middle wavelength channel with conventional DFT-S-OFDM (left) and for FTN-DFT-S-OFDM (middle, right).

To fill the other half of the spectrum, the half-spectrum was split into two paths; one path was frequency shifted by 8-GHz, amplified and recombined with the other path to form the complete super channel, shown as inset (ii). Polarization multiplexing was performed with a 19.6-ns delay between the polarizations. These dual-polarization signals were then transmitted through a recirculating loop with 560 km of standard single-mode fiber per loop. ASE noise was coupled in single-channel back-to-back scenario. Another WS was used to select the channels for coherent detection; finally, the signals were digitized by a real-time scope for offline DSP processing.

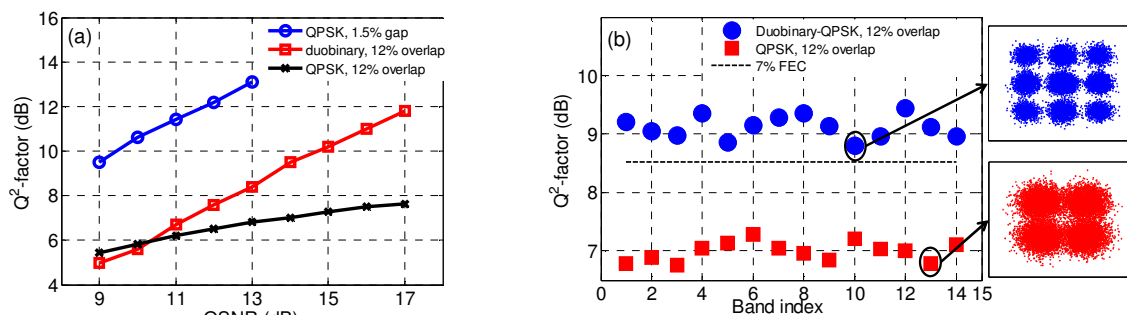


Fig. 3. Experimental results for: (a) single-channel back-to-back OSNR sweep, (b) after 3360-km transmission.

We compared three systems: conventional DFT-S-OFDM with 1.5% sub-band gap, FTN-DFT-S-OFDM with and without duobinary filtering both with 12% sub-band spectrum overlap. The receiver DSP included following procedures: (1) frequency and frame synchronization, (2) a DFT matched to the transmitter IDFT operation, (3) CD compensation, (4) two IDFTs matched to the transmitter DFTs to split and convert each sub-band to time domain, (5) overlap-add for serial to parallel conversion, (6), polarization de-multiplexing, (7) phase recovery. Same sub-band de-multiplexing (stages (1)-(5)) was used for all three systems, except that the IDFT size was different according to different overlap ratio. Stages (6) and (7) were applied to each sub-band separately: for the signals without duobinary filtering, a standard constant modulus algorithm and Viterbi-Viterbi phase estimation were employed [9]; for the duobinary-filtered signals, cascaded multi-modulus algorithm and two stage QPSK partitioning phase recovery [10] were used, with an extra 1-bit MLSE to make the decision [6].

Figure 3a plots the measured Q^2 -factors ($Q^2(\text{dB}) = 20 \log_{10}(\sqrt{2} \text{erfc}^{-1}(2\text{BER}))$), versus OSNR (0.1nm). Without duobinary filtering (black), the FTN-DFT-S-OFDM system performance is degraded and limited by strong ISBI; duobinary-shaping (red) mitigates this ISBI, providing improved Q^2 performance, the penalty induced by duobinary filtering is around 4-dB compare to conventional DFT-S-OFDM with a 1.5% guard band (blue curve).

Figure 3b shows the measured results of all 14 bands of FTN-DFT-S-OFDM system with 12% overlapped sub-band spectra after 3360-km transmission with optimal launch power (4 dBm). The combination of duobinary filtering and MLSE detection offers more than 2-dB Q^2 performance improvement compared to the overlapped system without duobinary filtering, and all sub-bands are above the 7% FEC threshold. After accounting FEC overhead, the net data rate is 502.4-GHz with 4.48-b/s/Hz spectral efficiency, compare to conventional super-channel, a 12% enhancement in terms of spectral efficiency is realized.

4. Conclusion

We report a digital FTN signal generation method based on overlapping the sub-bands of a conventional multi-band DFT-S-OFDM signal. The proposed method can precisely control the ISBI to adapt to the actual network scenarios, increase the per-channel symbol rate beyond the Nyquist bandwidth while maintaining zero inter-channel interference, at negligible computational cost. After combining with duobinary filtering and MLSE for ISBI mitigation, the proposed concept is experimentally demonstrated in a 14×38.4-Gb/s super-channel over 3360-km.

Acknowledgement

This work is supported by the Australian Research Council's Laureate Fellowship Grant (FL13010041).

References

- [1] G. Bosco, *et al.*, "Performance limits of Nyquist-WDM and CO-OFDM in high-speed PM-QPSK systems," *IEEE Photon. Technol. Lett.* **22**(15), 1129-1131 (2010).
- [2] A. J. Lowery, *et al.*, "Performance of optical OFDM in ultralong-haul WDM lightwave systems," *J. Lightw. Technol.* **25**(1), 131-138 (2007).
- [3] G. Colavolpe, *et al.*, "Faster than Nyquist and beyond: how to improve spectral efficiency by accepting interference," *Opt. Express* **19**(27), 26600-26609 (2011).
- [4] K. Igarashi, *et al.*, "Super-Nyquist-WDM transmission over 7,326- km seven-core fiber with capacity-distance product of 1.03 Exabit/s·km," *Opt. Express* **22**(2), 1220-1228 (2014).
- [5] Y. Tang *et al.*, "DFT-spread OFDM for fiber nonlinearity mitigation," *IEEE Photon. Technol. Lett.*, **22**(16), 1250-1252 (2010).
- [6] J. Li, *et al.*, "Approaching Nyquist limit in WDM systems by low-complexity receiver-side duobinary shaping," *J. Lightw. Technol.* **30**(11), 1664-1676 (2012).
- [7] L. B. Du, *et al.*, "DAC generated multi-channel Nyquist WDM," *Proc. of OECC 2014, Melbourne, Australia*, pp. 73-75, July 2014.
- [8] N. Kaneda, *et al.*, "Frequency diversity MIMO detection for coherent optical transmission," *Proceedings of ECOC 2013*, pp. 1-3, 2013.
- [9] C. Zhu, *et al.*, "Improved two-stage equalization for coherent Pol-Mux QPSK and 16-QAM systems," *Opt. Express* **20**(26), B141-B150 (2012).
- [10] J. Zhang, *et al.*, "Multi-modulus blind equalizations for coherent quadrature duobinary spectrum shaped PM-QPSK digital signal processing," *J. Lightw. Technol.* **31**(7), 1073-1078 (2013).